Model selection in kaon photoproduction

D. Skoupil, P. Bydžovský, A. Cieplý, D. Petrellis and D. Trnková

Nuclear Physics Institute - Řež, Czech Republic

received 21 December 2023

Summary. — We study photoproduction of kaons on protons within the framework of isobar model. Our models were constructed using consistent formalism for exchanges of high-spin resonances and with energy-dependent widths of nucleon resonances. For adjusting free parameters of the model to experimental data we employ regularization techniques, which prevent us from overfitting the data and help us select the appropriate model. We analysed the abundant data on the $K^+\Lambda$ channel as well as the recent data on $K^+\Sigma^-$ channel and show comparisons of the results with data.

1. – Introduction

The photoproduction and electroproduction of hyperons from nucleons are both promising processes for studying the spectrum of baryon resonant states. We may learn about the "missing resonances" predicted by quark models, which have not been detected in experiments with the π or η meson production probably due to their strong coupling to $K\Lambda$ and $K\Sigma$ channels. In order to better understand the hyperon–nucleon as well as hyperon–hyperon interactions, one may apply a description of the fundamental processes to the production of hypernuclei [1, 2].

In the last few decades, several theoretical studies of the hyperon production have been accomplished, focusing particularly on the $K^+\Lambda$ photoproduction. The first studies of this process date back to the 1960s. More experimental data became accesible in the 1980 s and 1990 s, allowing further theoretical studies to be carried out. The team at Ghent University analyzed the background contributions to the $K^+\Lambda$ photoproduction and the roles of contributing hyperon resonances [3]. They created a model describing the $p(\gamma, K^+)\Lambda$ at the threshold and at high energies [4, 5] utilizing the data on differential cross sections and polarization observables measured by the CLAS Collaboration [6]. Only a small amount of experimental data on differential cross sections obtained by using neutron targets are currently available [7-9]. The experiments measuring the beam asymmetry Σ in the $K^+\Sigma^-$ channel have been performed by the LEPS collaboration [7] and recently also by the CLAS Collaboration [10] covering a wide range of kinematics.

The isobar models based on effective Lagrangians are used to characterize the processes and the quantity of model parameters relates to the number of contributing resonances taken into account. Hyperon coupling constants take on unphysically high values in isobaric models, such as in the Saclay-Lyon model [11] or our models BS1 and BS2 [12], which were created in 2016 by using experimental data available at the time. In statistics, regularization techniques are frequently used to prevent overfitting and create models that describe the data more accurately. Recently, we have employed Ridge regularization to penalize large values of free model parameters. One can also use a specific set of resonances while shrinking the free model parameters by using Ridge regularization.

2. – Single-channel isobar model

In this work, the model of our choice for the kaon photoproduction study within the energy range from threshold up to 2.5 GeV is the single-channel isobar model. In this model, the reaction amplitude is constructed from effective meson-baryon Lagrangians as a sum of tree-level Feynman diagrams. The non-resonant part of the amplitude consists of exchanges of the ground-state hadrons and exchanges of kaon and hyperon resonances. The resonant part, then, is modelled by the exchanges of nucleon resonances. In this approach, we do not take into account contributions beyond the tree level such as rescattering and interaction in the final state. Since the exchanged particles have inner structure, we introduce a hadronic form factor in the strong vertex. The exchanges of nucleon resonances are the only ones which create resonant structures in the observables; the other diagrams contribute to the background part.

The most important novel features of the model are the consistent formalism for the exchange of high-spin resonances, where non-physical degrees of freedom, connected to the lower-spin content of the high-spin fermion fields, vanish in the amplitude, and the energy-dependent decay widths of nucleon resonances, which are introduced in order to restore unitarity.

Since in the kaon photoproduction there is no dominant resonance, we have to take into account *a priori* more than 20 resonances. This, unfortunately, results in a large number of possible resonance sets which describe the data reasonably well. In order to select the appropriate model from this large number of models, we employ model selection techniques.

3. – Model selection tools

Adjusting a theoretical model to experimental data involves seeking the values of the model parameters which minimize an error function. The use of complex models with large numbers of parameters usually leads to very low errors, even though it can make the minimization process unstable, resulting in many similar minima corresponding to varying values of the parameters. Therefore, limiting the magnitude and/or the number of the model parameters becomes crucial.

A most efficient tool for such cases is regularization which involves inclusion of a penalty term in the error function in order to prevent the parameters from taking extreme values. The penalty term consists of an L_q norm of the parameter vector and thus, in effect, converts the problem of error minimization to a problem of constrained minimization. We distinguish cases when $q = 1$ (L_1 norm) and $q = 2$ (L_2 norm), with the L_1 norm limiting both the number of parameters as well as their magnitudes and L_2 norm limiting only the magnitudes of parameters. The penalization with the L_2 norm gives

us Ridge regression with a smooth objective function but with poor parameter pruning ability. Using the L_1 norm, we obtain Least Absolute Shrinkage Selection Operator (LASSO) estimation technique that has good pruning behaviour but the non-smooth objective function causes optimization difficulties.

In this work, we made an upgrade of the fitting procedure for adjusting free parameters of the model. First, we opted for the LASSO method in order to minimize the amount of introduced parameters and thus avoid overfitting the data. We used this method together with information criteria in order to select the most appropriate model for the analysis of data in $K^+\Sigma^-$ [13] and $K^+\Lambda$ channels. Furthermore, we also made use of the Ridge regression in order to keep the couplings of resonances within their natural limits in the reanalysis of the data in the $K^+\Lambda$ channel.

4. – Results and discussion

We first focused on the channel with $K^+\Sigma$ in the final state and fitted the free parameters of the model to the available data. In the fit, we assumed around 20 parameters which were fitted to 674 data points. The result of the fitting procedure were two models: Fit M, which was achieved by minimizing the χ^2 with no regularization, and Fit L, which resulted from minimizing the penalized χ^2. In the Fit M, there are 25 parameters and 14 resonances, while in the Fit L there are only 17 free parameters and 9 resonances. The LASSO technique, thus, clearly leads to a more economical fit which is in a very good agreement with the experiment (in spite of the slight increase in the χ^2 value). Neither Fit M nor Fit L includes any hyperon resonances, which shows that their role for data description is rather small. Calculations of differential cross section $d\sigma/d\Omega$ and photon-beam asymmetry Σ by Fit M and Fit L are compared to data in figs. 1(a) and (b), respectively.

After employing the LASSO technique in the study of $K^+\Sigma^-$ channel, we focused on
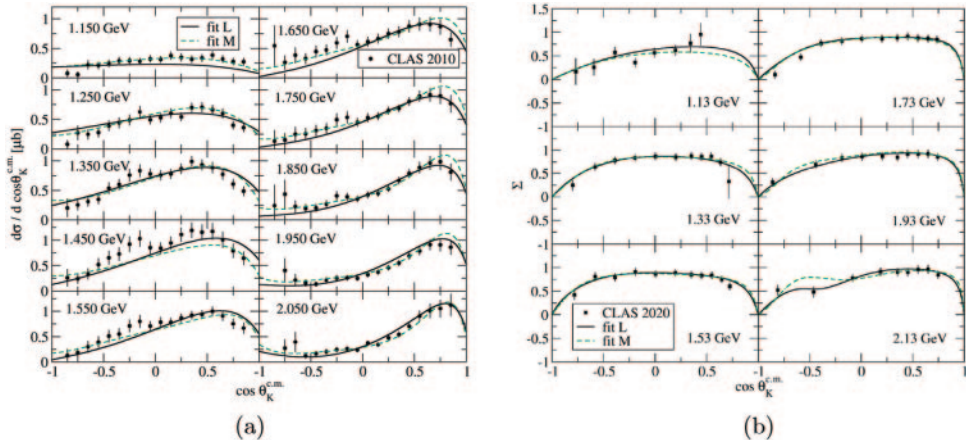

Fig. 1. – (a) The differential cross section of the $\gamma n \to K^+\Sigma^-$ process as a function of cosine of the kaon center-of-mass angle $\theta_K^{c.m.}$ for several photon lab energies E_γ^{lab}. The data are from ref. [8]. The fits L and M are represented by solid and dashed lines, respectively. (b) The photon-beam asymmetry of the $\gamma n \to K^+\Sigma^-$ process as a function of cosine of the kaon center-of-mass angle $\theta_K^{c.m.}$ for several photon lab energies E_γ^{lab}. The data are from ref. [10]. The fits L and M are represented by solid and dashed lines, respectively.
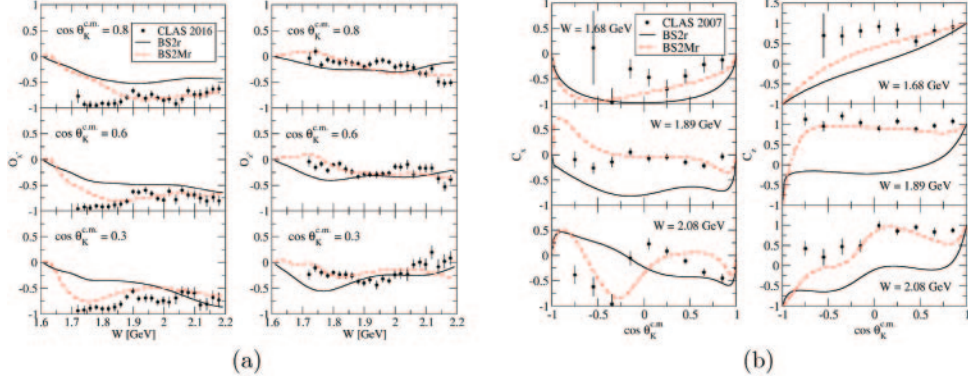
Fig. 2. – (a) Double-polarization asymmetries $O_{x'}$ and $O_{z'}$ of the $\gamma p \to K^+\Lambda$ process measured by CLAS [15] are compared to BS2r (solid line) and BS2Mr (dashed line). (b) Double-polarization asymmetries C_x and C_z of the $\gamma p \to K^+\Lambda$ process measured by CLAS [16] are compared to BS2r (solid line) and BS2Mr (dashed line).

the $K^+\Lambda$ channel using the Ridge regression technique. In this way, we could reduce the magnitude of hyperon couplings by one or two orders (for details see [14]). This analysis can shed a new light on the role and importance of hyperon resonances in the $K^+\Lambda$ photoproduction. Double-polarization asymmetries $O_{x'}$, $O_{z'}$, C_x, and C_z are shown in figs. 2(a) and (b) and compared to CLAS data [15, 16]. We see that the fit BS2Mr describes the data much better than the BS2r fit. The difference between these two fits is the replacement of $\Lambda(1800)1/2^-$ resonance in BS2r fit with $\Lambda(1600)1/2^+$ and with $\Lambda(1810)1/2^+$ in the BS2Mr fit. Therefore, the effect of hyperon resonances on data description still remains a subject of future studies.
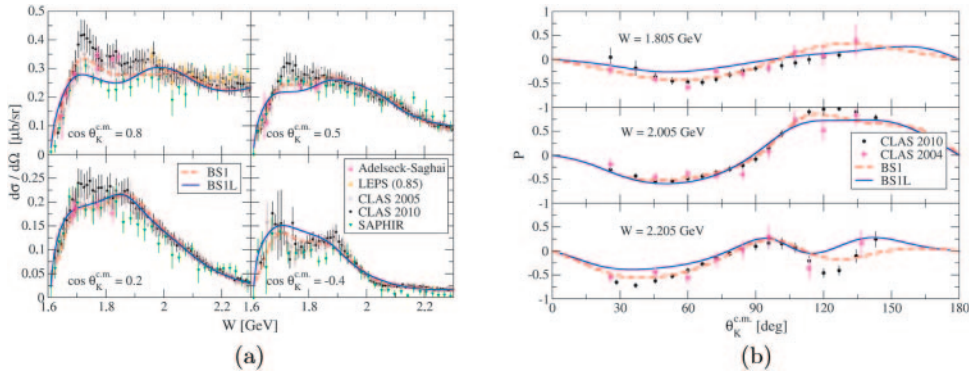

Fig. 3. – (a) The differential cross section of the $\gamma p \to K^+\Lambda$ process as a function of invariant energy W is shown for various cosines of kaon angles $\theta_K^{c.m.}$. Solid and dashed lines, respectively, illustrate the models BS1 and BS1L. The data stem from ref. [17], LEPS (for $\cos\theta_K^{c.m.} = 0.85$) [18], CLAS 2005 [6] and CLAS 2010 [19]. For comparison, also the SAPHIR data were added [20]. (b) The hyperon polarization asymmetry of the $\gamma p \to K^+\Lambda$ process as a function of the kaon center-of-mass angle $\theta_K^{c.m.}$ is shown for various invariant energies W. Solid and dashed lines, respectively, illustrate the models BS1 and BS1L. The data stem from collaborations CLAS 2010 [19] and CLAS 2004 [21].

In order to achieve an economical fit of the $K^+\Lambda$ channel, we employed also the LASSO regression technique in this channel. Similarly to the study with the Ridge regression, we were able to find a parsimonious fit which is in a good agreement with data and which does not include any hyperon resonances. The sparser model BS1L is based on the model BS1 and includes 9 resonances and 20 free parameters. Differential cross sections and hyperon polarization asymmetries described by the models BS1 and BS1L are illustrated in figs. 3(a) and (b) (although the results are still preliminary).

5. – Conclusion

We present description of the photoproduction of kaons on nucleons with help of the isobar model. The main novel features of our models are consistent interactions for exchanges of particles with spin larger than 1/2 and energy-dependent decay widths of nucleon resonances. In order to select the appropriate model and avoid overfitting, we opted for the regularization techniques. We compare behaviour of our new models with experimental data in the $K^+\Lambda$ and $K^+\Sigma^-$ channels. When we introduce the regularization techniques, which lead to more economical models with fewer parameters and resonances, we reveal that the role of hyperon resonances for reliable data description is rather small but non-negligible as they can affect model predictions in various kinematic regions.

REFERENCES

[1] Bydžovský P., Denisova D., Skoupil D. and Veselý P., *Phys. Rev. C*, **106** (2022) 044609.
[2] Bydžovský P., Denisova D., Petrellis D., Skoupil D., Veselý P., De Gregorio G., Knapp F. and Lo Iudice N., *Phys. Rev. C*, **108** (2023) 024615.
[3] Janssen S., Ryckebusch J., Debruyne D. and Van Cauteren T., *Phys. Rev. C*, **65** (2001) 015201; Janssen S. *et al.*, *Eur. Phys. J. A*, **11** (2001) 105.
[4] Corthals T., Ryckebusch J. and Van Cauteren T., *Phys. Rev. C*, **73** (2006) 045207.
[5] De Cruz L., Ryckebusch J., Vrancx T. and Vancraeyveld P., *Phys. Rev. C*, **86** (2012) 015212.
[6] Bradford R. *et al.*, *Phys. Rev. C*, **73** (2006) 035202.
[7] LEPS Collaboration (Kohri H. *et al.*), *Phys. Rev. Lett.*, **97** (2006) 082003.
[8] CLAS Collaboration (Pereira S. A. *et al.*), *Phys. Lett. B*, **688** (2010) 289.
[9] Tsukada K. *et al.*, *Phys. Rev. C*, **78** (2008) 014001.
[10] CLAS Collaboration (Zachariou N. *et al.*), *Phys. Lett. B*, **827** (2022) 136985.
[11] David J. C., Fayard C., Lamot G. H. and Saghai B., *Phys. Rev. C*, **53** (1996) 2613.
[12] Skoupil D. and Bydžovský P., *Phys. Rev. C*, **93** (2016) 025204.
[13] Bydžovský P., Cieplý A., Petrellis D., Skoupil D. and Zachariou N., *Phys. Rev. C*, **104** (2021) 065202.
[14] Petrellis D. and Skoupil D., *Phys. Rev. C*, **107** (2023) 045206.
[15] CLAS Collaboration (Paterson C. A. *et al.*), *Phys. Rev. C*, **93** (2016) 065201.
[16] CLAS Collaboration (Bradford R. K. *et al.*), *Phys. Rev. C*, **75** (2007) 035205.
[17] Adelseck R. A. and Saghai B., *Phys. Rev. C*, **42** (1990) 108.
[18] Sumihama M. *et al.*, *Phys. Rev. C*, **81** (2006) 035214.
[19] McCracken M. E. *et al.*, *Phys. Rev. C*, **81** (2010) 025201.
[20] Glander K. H. *et al.*, *Eur. Phys. J. A*, **19** (2004) 251.
[21] CLAS Collaboration (McNabb J. W. C. *et al.*), *Phys. Rev. C*, **69** (2004) 042201(R).